



Construction of an enzymatic biosensor for chlorpyrifos pesticide detection via acetylcholinesterase inhibition on oxidative boron-doped diamond electrode

Abdul Basit¹, Ferinastiti¹, Yudhistira Tesla², Fadlinatin Naumi^{3*}

¹ Department of Chemistry, Faculty of Mathematics and Natural Sciences, Universitas Indonesia, Depok, West Java 16424, Indonesia;

² Singota Solutions, Bloomington, Indiana 47401, United States;

³ Department of Chemical Engineering, Faculty of Engineering, Universitas Al-Khairiyah, Cilegon, West Java 42441, Indonesia.

*Correspondence: fnaumi@unival-cilegon.ac.id

ABSTRACT

Background: The extensive utilization of pesticides in agricultural practices presents considerable environmental and health hazards, which calls for the creation of precise and specialized detection techniques.

Methods: This study focuses on the development of an enzymatic biosensor designed to detect chlorpyrifos pesticide residues. The biosensor employs an oxidative boron-doped diamond (OBDD) electrode as the transducer platform, offering exceptional sensitivity and stability. The detection mechanism is based on the inhibition of acetylcholinesterase (AChE) activity on the OBDD surface. Various factors were optimized to assess the precision and sensitivity limit of the developed sensor. The cyclic voltammetry (CV) results indicated that the presence of AChE is necessary for acetylthiocholine chloride (ATCl) to generate an electrical signal. To enhance detection, AChE was modified with magnetic beads. **Findings:** This modification facilitated the oxidation of ATCl to thiocholine chloride, an oxidation peak of thiocholine could be observed at the magnetic beads modified AChE-Biotin/OBDD at a potential of +0.804 V (vs. Ag/AgCl), formed by an enzymatic reaction of AChE in the presence of acetylthiocholine. The current signal decreased due to the inhibition of AChE activity by chlorpyrifos pesticide. The oxidation current of thiocholine chloride consistently decreased as the chlorpyrifos concentration increased within the range of 0.001 nM to 10 nM at the optimum condition of 50 mM phosphate buffer solution pH 7.6; 250 μ g/5 mL AChE; and 1 mM ATCl in an inhibition and contact time of 30 and 15 min, respectively. The regression equation obtained using magnetic beads modified by AChE-Biotin is $y = 0.043 \ln(x) + 1.074$, with an R^2 value of 0.9062. The sensor demonstrated a lower limit of detection value of 0.6551 nM. **Conclusion:** Furthermore, the developed sensor proved suitable for testing real samples of tap water, showing minimal interference with a % RSD value lower than 10%. **Novelty/Originality of this Study:** This study introduces a novel enzyme-based biosensor using oxidative boron-doped diamond (OBDD) electrodes for detecting chlorpyrifos pesticide. The originality lies in the use of electrochemically modified BDD, which enhances enzyme immobilization and stability, providing higher sensitivity and lower detection limits compared to traditional methods.

KEYWORDS: acetylthiocholine chloride (ATCl); chlorpyrifos pesticide (CP); magnetic beads; oxidative boron-doped diamond electrode (OBDD).

1. Introduction

Organophosphorus pesticides are widely used globally as a safer alternative to the long-term and toxic organochlorine and carbamate group of pesticides. These pesticides are biodegradable compounds that exhibit lower environmental persistence and high

Cite This Article:

Basit, A., Ferinastiti, Tesla, Y., & Naumi, F. (2024). Construction of an enzymatic biosensor for chlorpyrifos pesticide detection via acetylcholinesterase inhibition on oxidative boron-doped diamond electrode. *Environmental and Materials*, 2(1), 12-28. <https://doi.org/10.61511/eam.v2i1.2024.890>

Copyright: © 2024 by the authors. This article distributed under the terms and conditions of the Creative Commons Attribution (CC BY) license (<https://creativecommons.org/licenses/by/4.0/>).



efficacy against a wide range of insect species (Das and Adhya, 2015; Nandhini et al., 2021; Gaonkar et al., 2019; Karpouzas and Singh, 2006; Kaur and Goyal, 2019). Chlorpyrifos (O,O-diethyl-O-3,5,6-trichloro-2-pyridyl phosphorothioate; CP) a non-systemic, broad-spectrum chlorinated OP insecticide that belong to the organophosphorus (OPs) family. The pesticides in question have been classified by the World Health Organization as a moderately hazardous class II pesticide. The half-life of chlorpyrifos in soil ranges from 20 to 120 days, with the formation of 3,5,6-trichloro-2-pyridinol (3,5,6-TCP) as the main degradation product. Other data indicate that the half-life can range from 2 weeks to more than 1 year. This high interchangeability of the half-life is related to the soil properties, which include the soil type, pH, moisture, temperature, organic matter and organic carbon content, and the microbial metabolism of chlorpyrifos (Jepson et al., 2020; Farsani et al., 2021; Nandhini et al., 2021). CP residues have been found in a variety of vegetables including eggplant, cabbage, cauliflower, ladyfinger (Sinha et al., 2012; Zhu et al., 2021). lettuce, carrot, and radishes (Yuan et al., 2014; Hongsihsong et al., 2020). They have also been detected in fruits like apples and pears (Jankuloska et al., 2016; Du et al., 2020). It is reported that CP is neurotoxic and has a negative impact on both immunological and psychological levels of health's (Nandhini et al., 2021). Acetylcholinesterase and cholinesterase play crucial roles in maintaining the proper functioning of the central nervous system (Rachmawati et al., 2023). CP disrupts the regular operation of these enzymes, leading to potential harm to the central nervous system as well as the sympathetic and parasympathetic nervous system (Hongsihsong et al., 2020; Yuan et al., 2014; Farsani et al., 2021).

Various analytical methods have been developed and utilized for detecting CP in various samples. There are several advanced techniques used in scientific research, such as high-performance liquid chromatography (Norbert Adum et al., 2021; Ramin et al., 2021). gas chromatography-mass spectrometry (GC-MS) (Tay and Wai, 2021), and liquid chromatography-mass spectroscopy (Lee et al., 2014; Jiao et al., 2022). While these methods are known for their accuracy and dependability, the process of preparing samples, conducting tests, and analyzing the results can be intricate and time intensive. The costs of the instrument are quite high, and typically require operators with specialized expertise (Rawtani et al., 2018), efficient, and cost-effective.

Electrochemical sensors are widely used for CP detection due to their excellent detectability, ease of use, and cost-effectiveness compared to other types of sensors (Dewi et al., 2024). Electrochemical biosensors can be categorized into different types, including voltammetry, conductometric, amperometry, potentiometric, and microelectromechanical systems (Zamora-Sequeira et al., 2019). Acetylcholinesterase (AChE) enzyme-based electrochemical biosensors have proven to be superior to previous methods for pesticide detection. They offer a low detection limit, rapid response, portability, and affordability (Nagabooshanam et al., 2019). AChE exhibited a high level of specificity and a strong affinity for the chlorpyrifos insecticide due to its abundant aromatic amino acid regions (Alex and Mukherjee, 2021).

For fabrication of stable and sensitive biosensors, the strategy for immobilization of the enzyme onto the electrode surface is one of the most important factors (Wei et al., 2014). Magnetic beads (MBs) modified with biomolecules have a wide range of applications in separation and sensing processes. The function of magnetic beads to immobilize AChE at an electrode surface. Modified magnetic beads have an advantage, as they provide a stable support for protein (AChE) immobilization and have been used successfully for ligand isolation for several proteins. Enhancing the affinity of MBs to the target molecule through modification by biomolecules (Williams et al., 2006; Wahyuni et al., 2016). Various carbon electrodes, including carbon nanotubes (Xue et al., 2012; Chauhan and Pundir, 2011), graphene (Yang et al., 2013), carbon spheres, porous carbon (Wei et al., 2014) have been utilized to immobilize AChE. The literature also mentioned the use of Indium Tin Oxide (ITO) (Nagabooshanam et al., 2019), Fluorine-doped Tin Oxide (FTO) (Talan et al., 2018), and Screen-Printed electrodes (SPEs) (Govindasamy et al., 2017) for electrochemical sensing of OPs. These electrodes present several challenges from a

commercialization perspective, such as high costs, the need for large sample volumes, surface imperfections, electrode fouling, and short shelf-life. Compared to the mentioned electrodes, the boron-doped diamond (BDD) electrode has superior fouling resistance, a small background current, a big potential window, and peculiar electrochemical characteristics (Wei et al., 2014; Rahmawati et al., 2024). The applications of BDD electrodes as detectors and sensors for some important pesticides especially have been reported. However, it is very rare that enzymatic systems have been developed using BDD electrodes, since it is difficult to perform chemical modifications, such as enzyme immobilization, at a BDD (Pino et al., 2015). Min Wei et al developed a novel AChE biosensor based on AuNPs-CSs nanocomposite for OPs detection. The prepared AChE/AuNPs-CSs/BDD biosensor exhibited higher sensitivity, lower detection limit, good reproducibility, and acceptable stability toward chlorpyrifos detection (Wei et al., 2014).

In this study, we present enzyme-based biosensors for the detection of chlorpyrifos pesticide. Oxidative boron doped diamond electrode (OBDD) electrodes were used because they have a wider working potential area compared to BDD. To obtain OBDD, oxidation of BDD electrochemically uses 0.1 M H_2SO_4 . At first cyclic voltammetry as much as 20 cycles was carried out in the potential range of -0.75 V to 1.75 V. Then, continue with chronoamperometry for 20 minutes at potential 3V. AChE and magnetic beads modified AChE that are immobilized on the OBDD were used to catalyze the hydrolysis reaction of acetylthiocholine chloride to thiocholine and acetic acid. The immobilized AChE exhibits greater affinity to its substrate and excellent catalytic effect on hydrolysis of ATCl. The proposed AChE biosensor is applied to detect chlorpyrifos pesticide as a model compound for OPs, and shows higher sensitivity, lower detection limit, quantification limit and acceptable stability. The developed sensor could apply in real tap water samples.

2. Methods

2.1 Materials and instruments

The chemicals and materials that were used in this research are, K_2HPO_4 (99.9%), KH_2PO_4 (99.9%), α -alumina, acetylcholinesterase (AChE, electrophorus electricus, EC 3.1.1.7), acetylthiocholine Chloride (ATCl, 99%), acetylthiocholine Iodide (ACTI, 99%), bovine serum albumin (BSA), and sulfo-NHS-biotin, H_2SO_4 (98%), NaOH, phosphate buffer saline (PBS), methanol (99.8%), glycerol ($\geq 99\%$), isopropanol ($\geq 99.8\%$), chlorpyrifos, and the solids magnetic beads. All the chemicals were analytical grade and purchased from Sigma-Aldrich. The instruments used in this experiment include Fourier Transform Infrared Spectroscopy (FTIR), X-Ray Photoelectron Spectroscopy (XPS), Scanning FEI Quanta 650 electron microscopy (SEM) and HORIBA - The LabRAM HR Evolution Raman Microscopes.

2.2 Fabrication of boron-doped diamond (BDD) electrode

OBDD were used as a working electrode for immobilization of enzymes. Prior to acquiring an OBDD electrode, it is advisable to conduct hydrogenated boron-doped diamond (HBDD) synthesis initially utilizing the Microwave Plasma Assisted Vapor Deposition (MPACVD) instrument. The process of synthesizing the HBDD electrode involves seeding and deposition. The seeding process involves gently scraping the surface of the silicon wafer onto the nanodiamond powder for about 20 minutes. This creates numerous scratches on the silicon wafer which facilitate the growth of crystals on the surface of silicon wafers. After the silicon wafers have been etched, they are carefully sonicated with isopropanol three times, each time for a duration of 5 minutes. Next, place the silicon wafer into the plasma chamber during the MPACVD process.

The basic principle of the MPACVD instrument is to deposit chemical vapors that have a duration of 6 hours. The diamond deposition process entails introducing carbon vapor

derived from methane gas (CH_4) into a hydrogen atmosphere at high pressures and temperatures. In addition, a small quantity of boron gas obtained from tri-methyl borate is added to assist in the process of doping boron onto the diamond. The general schematic can be seen in Figure 1 (Ivandini et al., 2019).

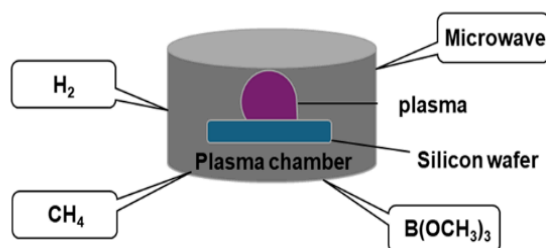


Fig. 1. MPACVD general scheme

A vibrant shade of purple plasma is created in the plasma chamber. When carbon vapor is introduced, an intense purple plasma with a noticeable yellow hue emerges on the surface of the silicon wafer. The plasma is ignited to initiate a nucleation process on the surface of the silicon wafer, leading to the creation of stable diamond sp^3 . BDD is formed by utilizing HBDD with the boron doping level of 0.1%. To obtain OBDD, HBDD was electrochemically oxidized using a 0.1M H_2SO_4 solution. The activation was achieved by performing cyclic voltammetry 20 cycles within the potential range of -0.75 V to 1.75 V followed by chronoamperometric test for a duration of 20 minutes, applying a potential of 3V (Ivandini et al., 2019). It was then subjected to a sonication process using isopropanol and aquabidest for 10 minutes each.

2.3 Measurement procedure

OBDD electrode was used as a working electrode and cyclic voltammetry technique was used for all the electrochemical experiments. Firstly, 0.1M phosphate buffer solution (PBS) (pH 7.4) was prepared, and acetylcholine chloride (ATCl) was immersed as a substrate to evaluate and study electrochemical signals generated by CV. AChE, AChE-Biotin Enzyme with Magnetic Beads and CP solutions prepared in 0.1M PBS were mixed and given them incubation time. After specific incubation time, the solution was immersed in the acetylthiocholine chloride solution.

The oxidation peak current obtained during the hydrolysis of acetylcholine chloride to thiocholine is related to the activity of immobilized AChE in the presence of chlorpyrifos pesticide. This could be used as an indicator for the quantitative measurement of the inhibition action of CP on the activity of immobilized AChE. The performance of the sensor was tested in the range of 0.001 nm to 10 nm chlorpyrifos concentration. For the real sample tap water was utilized and the effect of the interference analyte in tap water was investigated.

3. Results and Discussion

3.1 Characterization of BDD electrode

A study was conducted using Raman spectroscopy to analyze the chemical structure and molecular interactions of an OBDD. Prior to the characterization, it is necessary to lower the Raman instrument temperature to $-75\text{ }^\circ\text{C}$. Before using the sample, the Raman instrument is calibrated using naphthalene, a standard with known peaks. The BDD electrode was carefully positioned under the Raman instrument to precisely direct the laser beam onto the sample surface. The Raman spectrum displays peaks at 522 cm^{-1} , 1150 cm^{-1} , and 1333 cm^{-1} , as illustrated in Figure 2a.

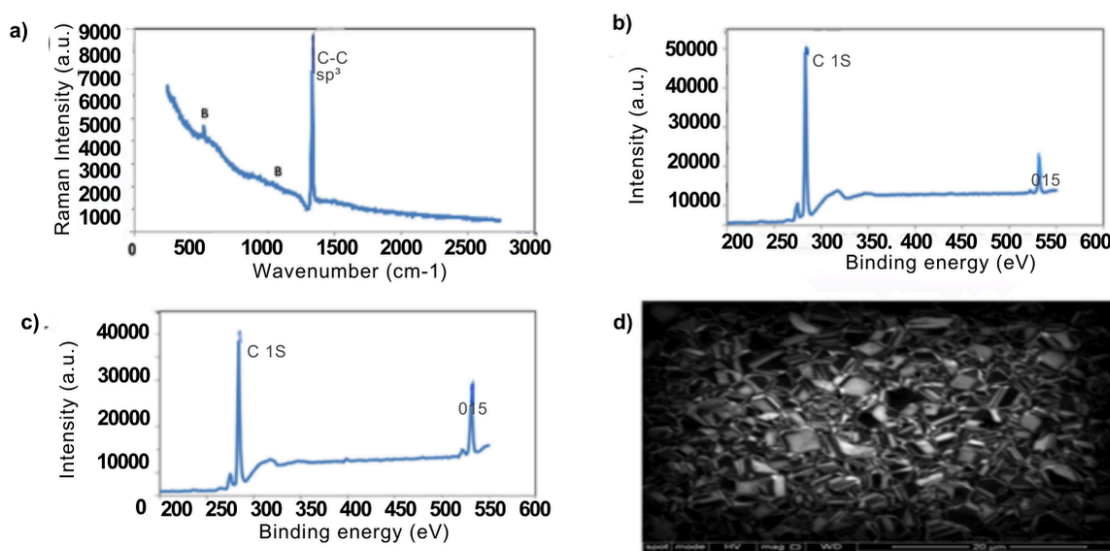


Fig. 2. (a) Raman study of BDD (b) XPS spectrum of an electrode OBDD (c) XPS spectrum of an electrode HBDD (d) SEM study of OBDD

There was a distinct peak at 522 cm^{-1} that corresponded to the Silicon signal. The peaks at 522 cm^{-1} and 1150 cm^{-1} exhibit the Fano effect. This effect demonstrates a correlation with B doping, indicating the coupling between phonons and electrons. This peak can also arise from the electronic interaction of excited boron. The diamond (C sp^3) crystal signal is indicated by a distinct peak at 1332 cm^{-1} . As the boron concentration increases, the sp^3 diamond peak decreases (Ivandini and Einaga, 2017).

The OBDD XPS spectra show a peak at bond energies of 284, 286 and 532 eV (Figure 2(b)). The bond energy 284 eV gives indication of the presence of C-H bond. The existence of C-C bonds at 286 eV peak and C-O and O-H bonds at 532 eV peak are indicative of the presence of these bond types on the surface of OBDD. The peak at 532 eV, a relatively high bond energy, indicates that OBDD was successfully synthesized with the oxygen-to-carbon ratio of 4:6. A peak at bond energies of 284, 286, and 532 eV was likewise produced in the XPS HBDD spectral data (Figure 2(c)) (Ivandini et al., 2019). Despite that, the peak is significantly lower than OBDD's at an O/C ratio of 2 to 9. Air or oxygen gas used in MPACVD contamination of HBDD could lead to the existence of an O group.

Micrographic images of the sample are captured using a Scanning Electron Microscopy (SEM) instrument. Figure 2(d) shows the results of BDD characterization using SEM tools. When magnified 6000 times, the diamond particles on the silicon wafer surface measure approximately $2.5\text{ }\mu\text{m}$ in size. The figure clearly demonstrates the high level of homogeneity in the BDD size, which is indicative of excellent BDD quality.

3.2 Modification of AChE enzyme with sulfo-NHS-biotin

Modification of AChE enzyme with sulfo-NHS-biotin has been added to the AChE enzyme during its preparation. Immobilizing the AChE enzyme on electrodes requires altering the enzyme therefore it may be attached to magnetic beads that have been treated with avidin. Filtering to remove buffer-tris from the AChE enzyme is required prior to making modifications with Sulfo-NHS-Biotin. The reason behind this is that the tris-amine buffer's group can hinder Sulfo-NHS-Biotin's ability to attach to the AChE enzyme. Competitors for binding to the AChE enzyme include buffer-tris and sulfo-NHS-biotin.

The desalting process utilizing the PD-10 column involves a series of precise steps to effectively exchange the tris-buffer, as presented in Figure 3. Following the removal of the PD-10 column from the carrier solution, thorough rinsing with PBS at pH 7.6 is performed to eliminate any residual carrier solution. Subsequent loading of the AChE enzyme onto the

PD-10 column isolates its tris-buffers, while a pre-prepared sulfo-NHS-biotin solution lies beneath to facilitate interaction. After transfer to a sulfo-NHS-biotin-containing container, a 12-hour incubation period at room temperature allows for optimal enzyme reaction. Reintroduction into the PD-10 column removes any remaining buffer-tris, followed by storage of the desalted findings at 4°C in a solution of 50 mM PBS, 1 mg/mL BSA, and 50% glycerol to maintain enzyme stability. Storage in glycerol at a 50% concentration preserves the AChE biotin enzyme's activity over time.

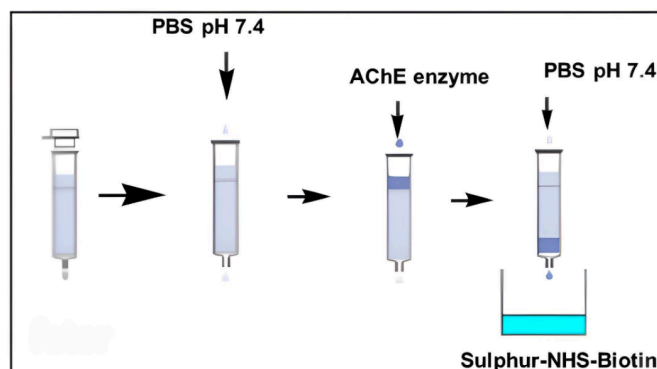


Fig. 3. Illustration of the use of the PD-10 column

3.3 Modification of AChE-Biotin enzyme with magnetic beads

The successful conjugation of AChE-Biotin enzyme with magnetic beads is achieved through meticulous steps shown in Figure 4(a).

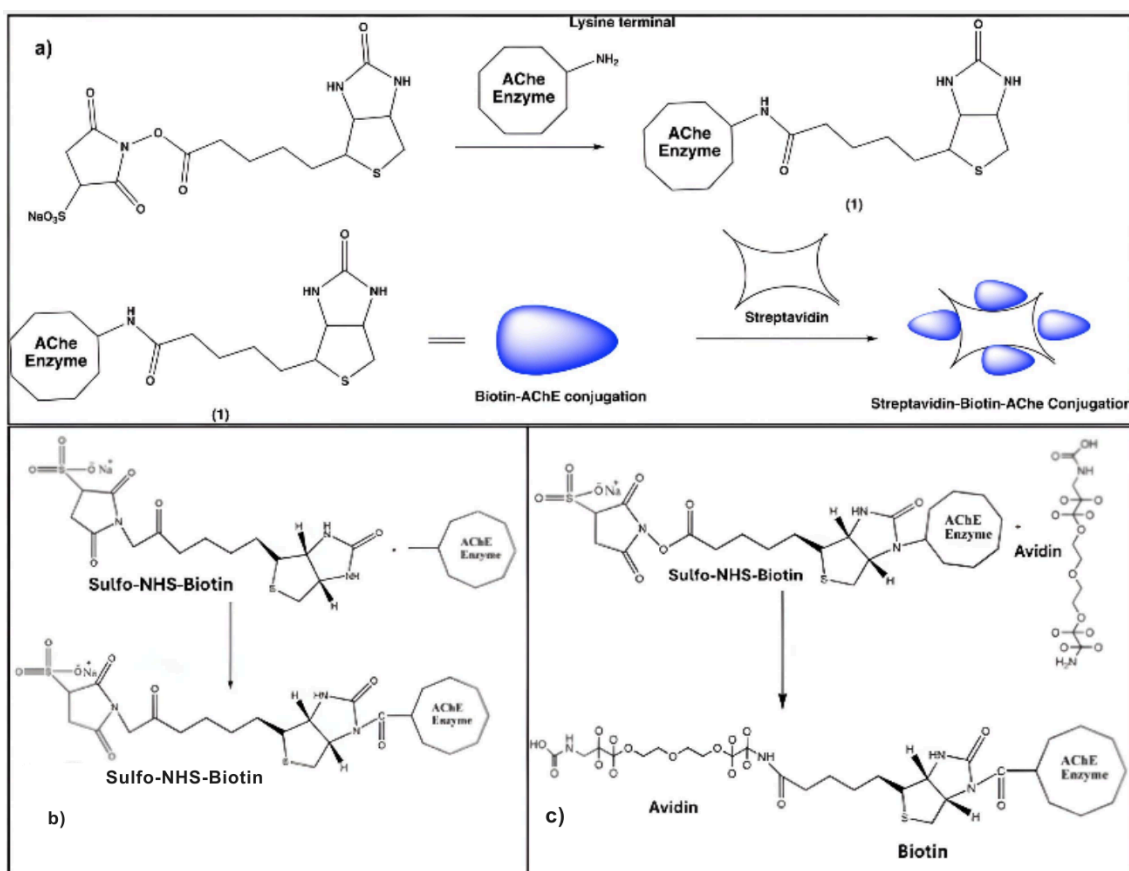


Fig. 4. (a) Illustration of AChE-biotin enzyme modified with magnetic beads (b) Reaction of AChE enzyme with sulfo-NHS-biotin (c) Reaction between enzyme-biotin and avidin

These beads, structured like colloids with metal nanoparticles and modified with avidin, are homogeneously prepared and then separated from the carrier solution using magnetic shelves. Thorough cleansing with PBS ensures bead purity before the enzyme is attached through gentle agitation and subsequent 12-hour incubation at 4°C. The interaction between AChE enzyme and Biotin likely occurs at specific chemical groups, such as the lactam group in sulfo-NHS-biotin and the carboxyl group in AChE, forming stable covalent or hydrogen bonds (Figure 4(b)). This attachment mechanism is similar to the specific binding observed in studies utilizing avidin modified magnetic beads (Figure 4(c)), highlighting the efficacy of such conjugation methods in biochemical research.

3.4 Electrochemical study of acetylthiocholine iodide (ACTI) with acetylthiocholine chloride (ATCl)

Electrochemical characteristic of thiocholine on the electrode was determined using cyclic voltammetry (CV) method. The electrochemical activity of iodide ions is demonstrated by the oxidation peaks at a potential of +1.104 V, as shown in Figure 5(a), which is derived from cyclic voltammetry (CV) observations.

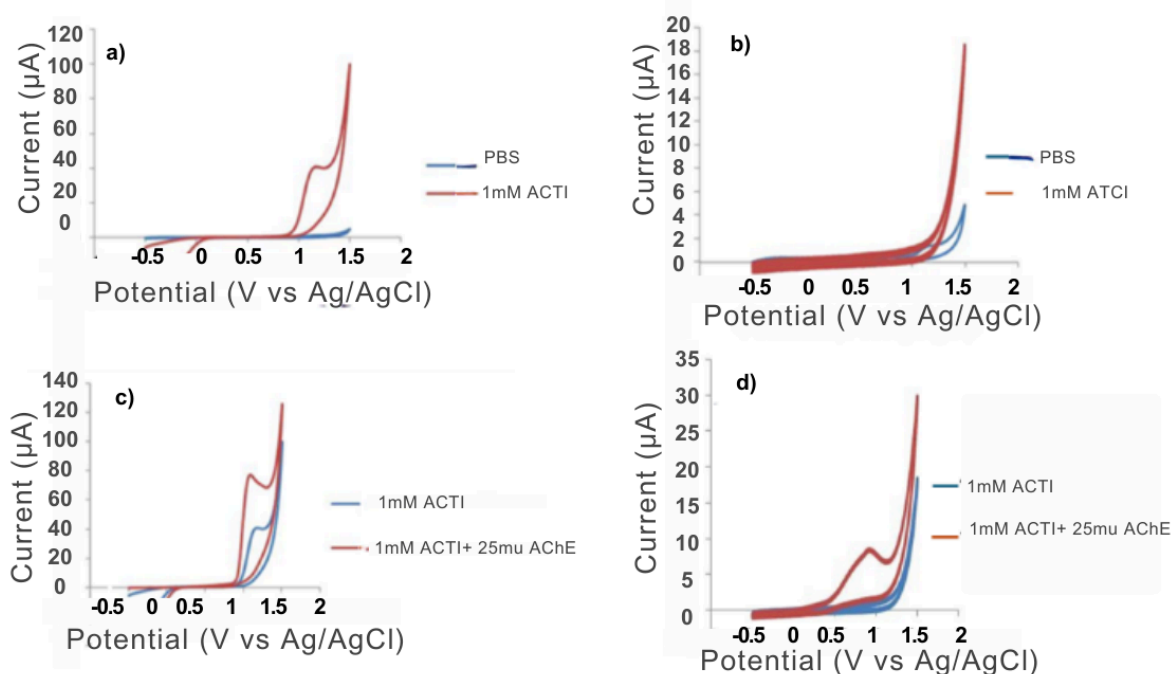


Fig. 5. (a) CV 1mM ACTI (b) CV 1mM ATCl (c) CV 1mM ACTI with 25mU AChE (d) CV 1mM ATCl with 25mU AChE

As shown in Figure 5 (a) ACTI does show an electrical signal, which represents the oxidation reaction of the iodide ion. In contrast, no electrochemical activity is observed when measuring ATCl with CV, resulting in no signal shown in Figure 5 (b). The distinction between ATCl and ACTI in peak oxidation potential is due to the fact that iodide ions are more easily oxidized than chloride ions. This is clearly demonstrated by the oxidation potential of iodide and chloride ions. The oxidation potential of iodide ions is +0.54 V and chloride ions is +1.36 V. The response of ACTI is further enhanced by the addition of AChE, as shown in Figure 5 (c), resulting in an increased formation of thiocholine. The addition of AChE enzyme to ATCl also catalyzes the oxidation of thiocholine chloride at a potential of about +0.804 V, which was not previously observed without the AChE enzyme (Figure 5 (d)). Based on this voltammogram study, ATCl exhibited a more selective oxidation peak potential for thiocholine compared to ACTI.

3.5 Determination of the optimum condition

It is important to optimize several factors to get accurate and precise results. pH could affect the enzymatic activity of the AChE; therefore, it is important to optimize the pH of the solution. The pH of the solution was optimized using CV method by applying varying pH from 7.0 to 7.8. The measurement is done by mixing 25 mU AChE, 1 mM ATCl, and 50 mM PBS with varying pH. As shown in the Figure 6(a) and (b), The hydrolysis of ATCl into thiocholine increases, as indicated by a gradual increase in the oxidation peak current with increasing pH up to 7.6. Further increases in pH have no effect on the oxidation peak current of thiocholine and pH 7.6 was chosen as the optimum pH for further observations.

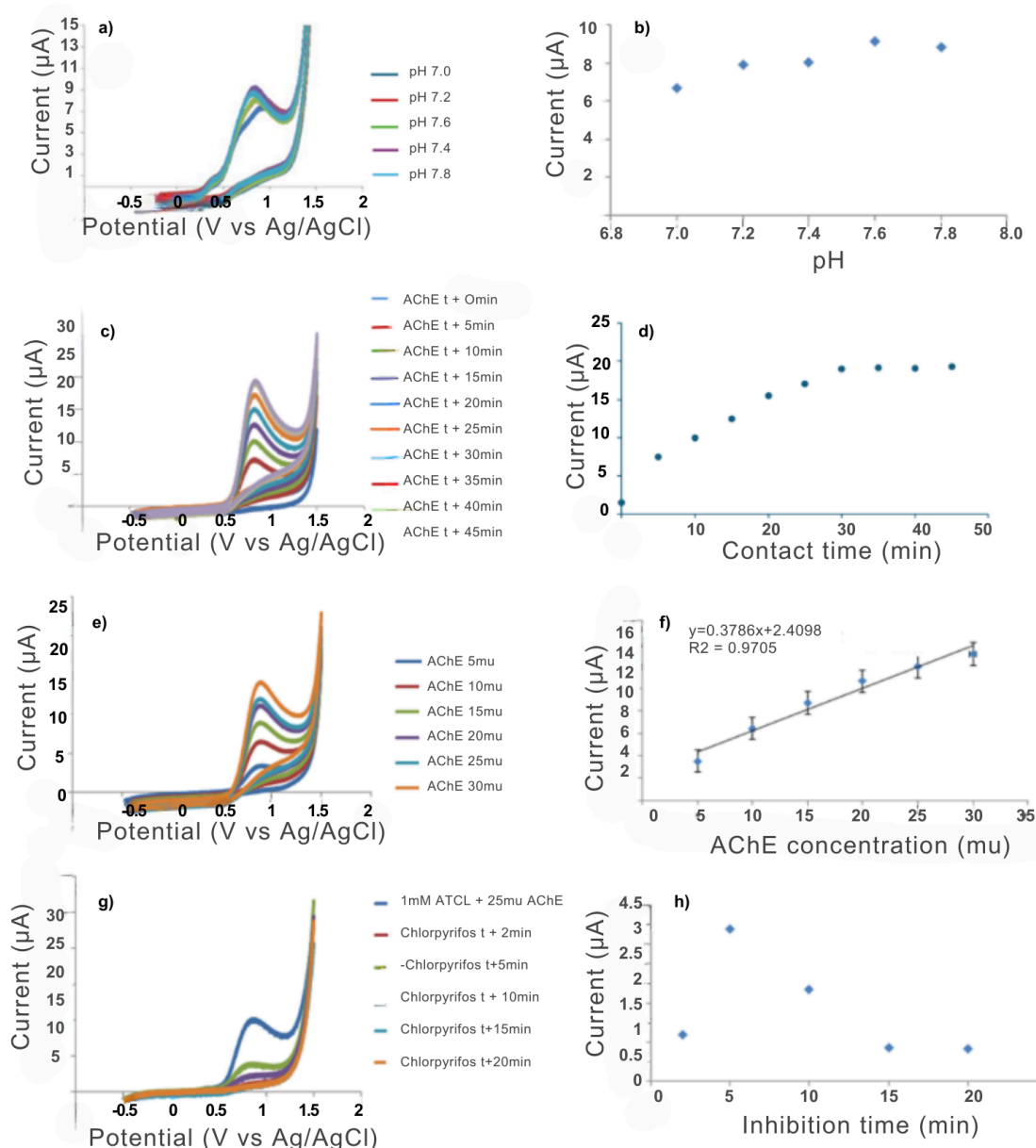


Fig. 6. (a) and (b) optimization of pH, (c) and (d) optimization of contact time between AChE and acetylthiocholine chloride, (e) and (f) optimization of concentration of AChE, (g) and (h) determination of the optimum inhibition time

The optimal time for determining the activity of AChE enzyme was examined in a 50mM solution of PBS pH 7.6 mixed with 1mM ATCl. The time duration ranges from 5 minutes to 45 minutes, with intervals of 5 minutes. As shown in Figure 6 (c) and (d) the contact time being observed is the duration of interaction between AChE and ATCl. Based on the measurement results, it can be observed that the current response gradually increases as the contact time increases, reaching its peak at 30 minutes. During a contact time of 30 minutes to 45 minutes, the current response remains consistent. Thus, the ideal contact time is 30 minutes.

The relationship between AChE enzyme concentration and oxidation peak current of thiocholine was studied using CV at optimum contact of 30 min and optimum pH of 7.6 (Figure 6. (e) and (f)). The measurement was taken using various concentrations of AChE enzyme ranging from 5mU to 50mU with an interval of 5mU and 1mM ATCl on the surface of the OBDD electrode. The increasing concentration of AChE enzymes gradually increases the peak oxidation current of thiocholine which is directly related to the production of thiocholine in the reaction system. The linear regression equation was as follows $y = 0.3786x + 2.4098$. The limit of detection (LOD) value for AChE detection on the OBDD electrode using straight line equation is 1.777316 mU. The limit of quantification (LOQ) is 5.9243mU and the sensitivity is 2.4098 μ A/mU.

The duration of AChE enzymatic activity inhibition by chlorpyrifos pesticide was evaluated using CV method. It was found that the current response decreases as chlorpyrifos inhibits the enzyme activity of AChE at the surface of the OBDD electrode. The observed variation in inhibition time ranged from 5 to 20 minutes, with intervals of 5 minutes, as depicted in Figure 6 (g) and (h). The current response is minimal after 2 minutes of inhibition time. This is because the ATCl were not mixed well with the solution, resulting in a limited production of thiocholine. After 5 minutes of inhibition time, the current response increases in comparison to 2 minutes of inhibition time, as the enzyme activity begins to take effect. Nevertheless, with an inhibition time of 5 minutes, there is a noticeable decrease in current when compared to the background, which consists of a mixture of ATCl and AChE enzymes in a PBS solution. The current peaks that can be observed at a potential of +0.825 V, decrease further as the inhibition time increases. The current response at an inhibition time of 15 minutes appears to be consistently stable. Thus, the time for inhibiting subsequent studies was set at 15 minutes.

3.6 Performance of the sensor

3.6.1 Linear calibration curve of chlorpyrifos pesticide

The performance of the sensor was examined using AChE and magnetic beads modified AChE-Biotin. The measurement was carried out at optimum inhibition time of 15 minutes and optimum contact time of 30 minutes using LSV method. As shown in the Figure 7 (a) and (b) visible peak at +0.787V observed for AChE/OBDD which corresponds to the oxidation of thiocholine.

Similarly, for magnetic beads modified by AChE-Biotin, the thiocholine peak was observed at a potential of +0.813 V (Figure 7 (c) and (d)). It was discovered through observations that the decrease in current due to concentration variations is relatively small in comparison to the unmodified AChE system. The values of IC₁₀ and IC₅₀ was determined by inputting the corresponding inhibition percentages of 10% and 50% as the values of y into the linear equation $y = 0.054\ln(x) + 1.248$ for AChE system and $y = 0.043\ln(x) + 1.074$ for magnetic beads modified AChE-Biotin system. The equations yield an IC₁₀ value of 0.0005nM and an IC₅₀ value of 0.9643nM for non modified AChE system and IC₁₀ value of 0.0001nM and an IC₅₀ value of 1.5947nM for magnetic beads modified AChE-Biotin system.

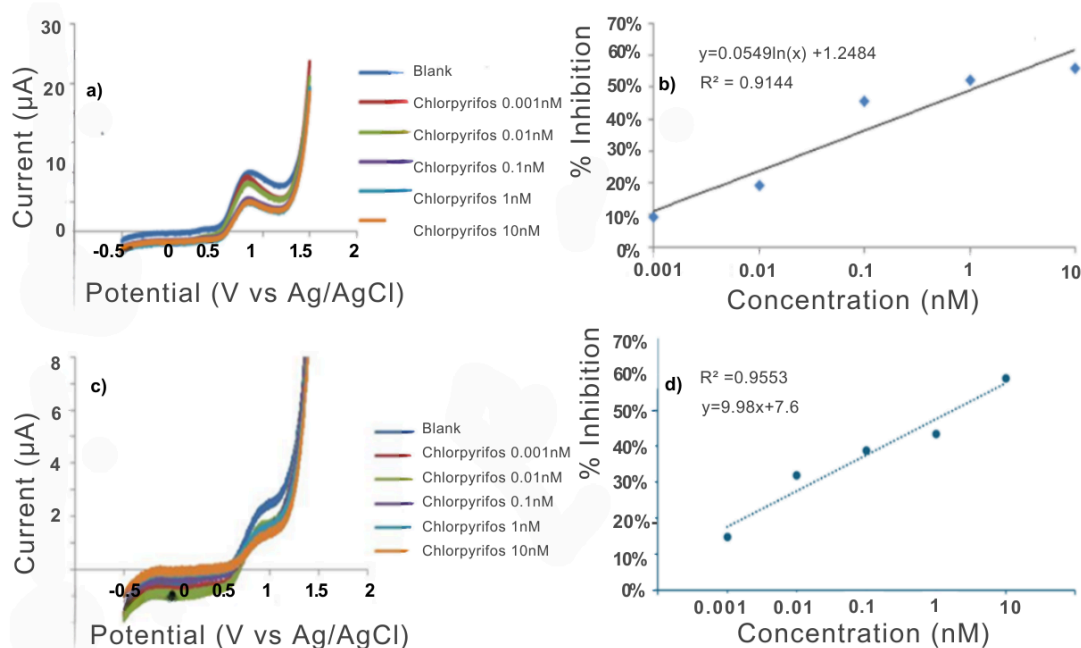


Fig. 7. (a) and (b) linear calibration curve of non modified AChE/OBDD (c) and (d) linear calibration curve of magnetic beads modified AChE-Biotin/OBDD for chlorpyrifos analysis

LOD values calculated for non modified AChE is 12.0204 nM and for magnetic beads modified AChE-Biotin is 0.6551 nM. Modified enzyme systems exhibit greater sensitivity compared to unmodified enzyme systems. The range of IC₁₀ and IC₅₀ in AChE-biotin mobilized in magnetic beads is wider compared to the range of IC₁₀ and IC₅₀ in AChE that is not mobilized. A comparison with other reported chlorpyrifos biosensors based on AChE is presented in Table 1.

Table 1. Comparison with other reported chlorpyrifos biosensors based on AChE

Analytical method	Linearity range	Detection limit	Quantification limit	Reference
Chemiluminescence CL	10-1000 ng/mL	3.50 ng/mL	3.5000 ng/mL	(Li et al., 2008)
GCF	0.20-250.00 ng/mL	0.04 ng/mL	0.04 ng/mL	(Pelit et al., 2012)
SERS	0.001-1000 mg/L	1.00 mg/L	1.00 mg/L	(Ma et al., 2020)
SERS-AuNPs	0.01 -10 mg/L	10.00 μg/L	10 μg/L	(He et al., 2019)
AuNPs-CSs modified BDD	10 pM-10 μM	13.00 pM	13 pM	(Wei et al., 2014b)
Tyr/nano-Pt/graphene/GCE	0.7 nM-29 nM	0.57 nM	0.57 nM	(Liu et al., 2011)
AChE-MB/BDD	10-1000 ng/mL	0.65 nM	0.6551 nM	This work

Abbreviation: (CL) Chemiluminescence; (GCF) gas chromatography; (SERS) surface-enhanced Raman spectroscopy; (SERS-AuNPs) surface-enhanced Raman spectroscopy with gold nanoparticles; (AuNPs-CSs modified BDD) boron-doped diamond electrode modified with gold nanoparticles and carbon spheres; (Tyr/nano-Pt/graphene/GCE) glassy carbon electrode modified with graphene and tyrosinase immobilized on platinum nanoparticles; (AChE-MB/BDD) Acetylcholinesterase modified magnetic beads on boron-doped diamond electrode

3.6.2 Stability of the sensor

In stability measurements, 3 scans were conducted with pesticide concentrations of 0.001 nM, as illustrated in Figure 8 (a), (b), (c), and (d). The stability measurement yielded a %RSD of 8.5031%, which falls within the acceptable range for electrochemistry.

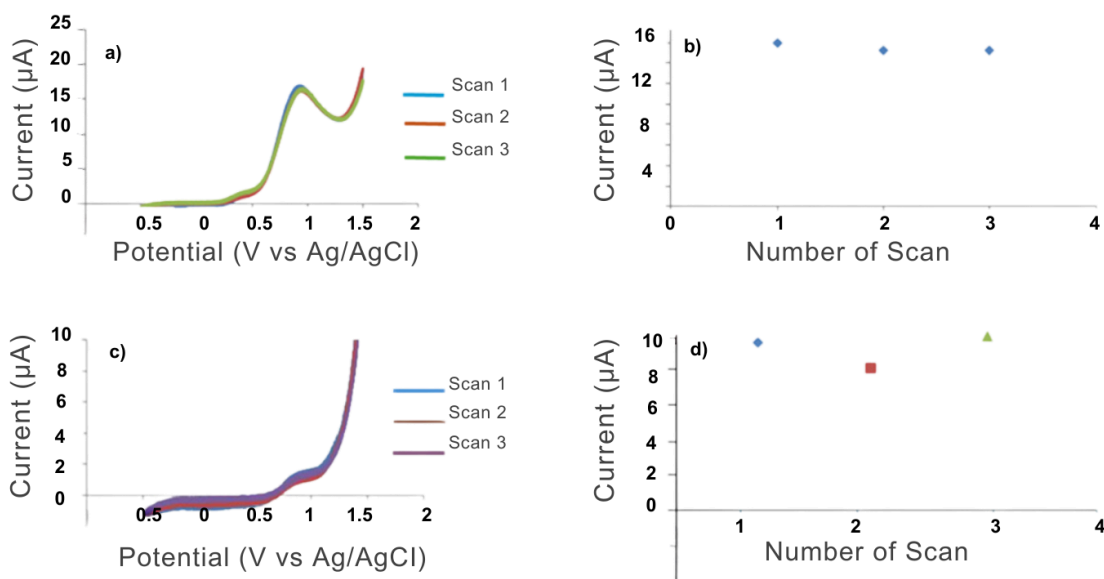


Fig. 8. (a) and (b) stability study of non-modified AChE/OBDD (c) and (b) stability study of magnetic beads modified AChE-Biotin/OBDD for chlorpyrifos analysis

3.6.3 Applications of the developed sensor in tap water sample

The linearity and selectivity of the sensor in tap water were tested by measuring the variation in pesticide concentration using AChE and AChE-Biotin modified magnetic beads. As shown in Figure 9 (a) and (c) an observation was made of a peak of thiocholine at a potential of +0.796 for AChE and V +0.874 V for AChE-MBs. The current response in tap water without the addition of pesticide showed a slight decrease, indicating that the sensor has minimal interference from other analytes present in the tap water, as depicted in the Figure 9 (a), (b), (c), and (d).

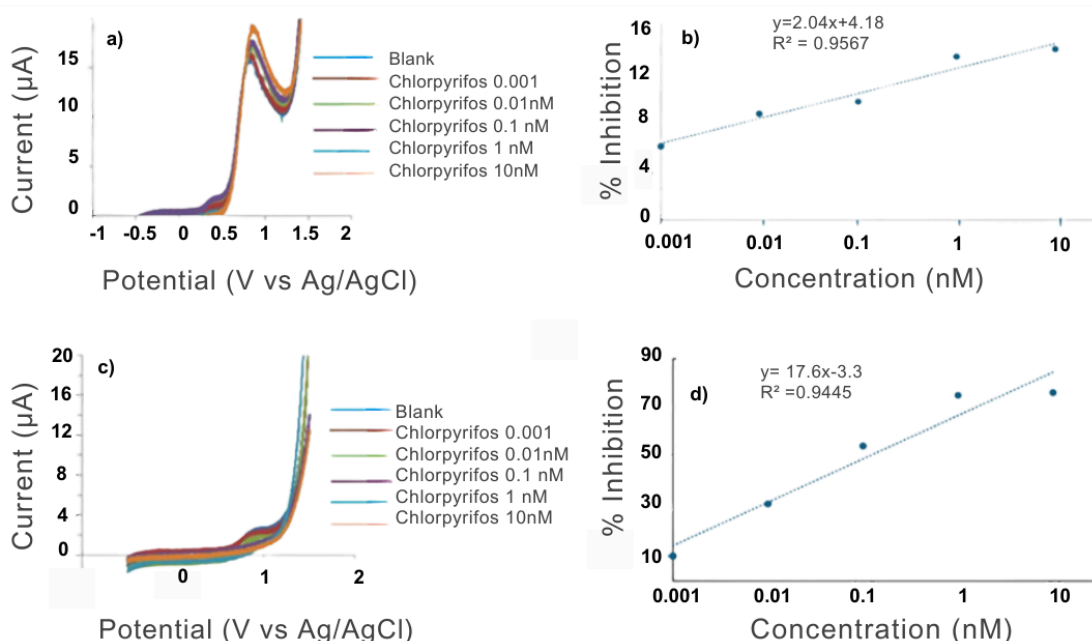


Fig. 9. (a) and (b) application of the sensor in real tap water using non modified AChE/OBDD (c) and (d) application of the sensor in real tap water using magnetic beads modified AChE-Biotin/OBDD for chlorpyrifos analysis

The IC₁₀ and IC₅₀ values were calculated, that is IC₁₀ value 0.0005 nM and an IC₅₀ value of 0.0986 nM AChE-MBs. According to the measurements, the obtained data remains linear, but the sensitivity decreases, indicating the impact of tap water interference. This is evident in AChE-MBs where tap water is not utilized. The IC₁₀ and IC₅₀ values have a broader range compared to those obtained using tap water.

3.7 Possible reaction mechanism of the developed sensor

Figure 10 (a) and (b) explain the mechanism of enzymatic hydrolysis of acetylthiocholine that occurred in the active site of AChE with acetylthiocholine quaternary nitrogen atom is bound to AChE anionic site and carboxyl group to esteratic site of AChE to produce thiocholine and acetic acid (Rachmawati et al., 2023). The serine group of acetylcholinesterase contain the hydroxyl group that act as a strong nucleophile and may attack on the phosphorus group of chlorpyrifos molecules the bound the chlorpyrifos molecule to the hydroxyl group on the AChE serine active site to inhibit the AChE catalytic activity.

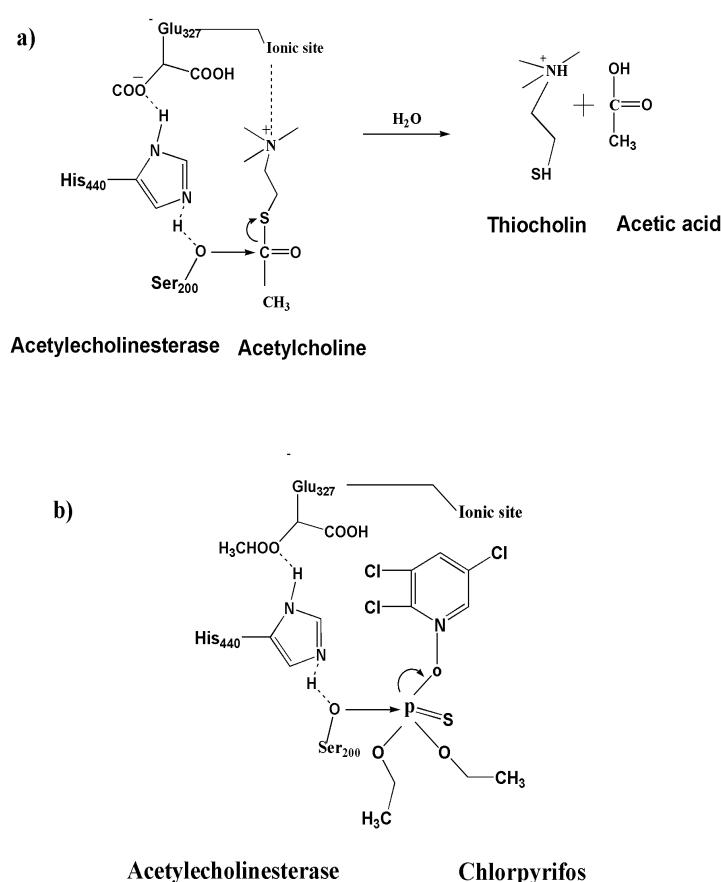


Fig. 10. (a) Reaction mechanisms of acetylthiocholine hydrolysis by AChE active sites, and (b) AChE inhibition by chlorpyrifos

4. Conclusions

In this work, we demonstrated a low cost and simple pesticide residue method using magnetic beads modified AChE-Biotin that is immobilized on a OBDD electrode. The developed sensor exhibits good performance towards chlorpyrifos pesticide residue detection and gives a linear decrease in the thiocholine current in the range of 0.001nM to 10nM. The regression equation obtained using magnetic beads modified by AChE-Biotin is $y = 0.043\ln(x) + 1.074$, with an R^2 value of 0.9062. The developed sensor gives a LOD value of 0.6551nM which is compatible with other enzymatic sensors. The sensor is applicable in

the real tap water sample and gives high stability towards the chlorpyrifos detection. There is a low decrease in the sensitivity in the tap water because of the presence of interference analytes.

Acknowledgement

Not available.

Author Contribution

Conceptualization, F.N.; Methodology, Y.T.; Validation, F.N., Y.T.; Formal Analysis, A.B., F.; Investigation, F.; Resources, Y.T.; Data Curation, A.B., F., Y.T.; Writing – Original Draft Preparation, A.B.; Writing – Review & Editing, F.N.; Visualization, A.B., F.; Supervision, F.N.

Funding

This work has been funded by the Ministry of Education and Culture, Directorate Higher Education, Republic of Indonesia, Hibah PDD 2021 with Contract No. NKB-318/UN2.RST/HKP.05.00/2021.

Ethical Review Board Statement

Not applicable.

Informed Consent Statement

Not available.

Data Availability Statement

Not available.

Conflicts of Interest

The authors declare no conflict of interest.

Open Access

©2024. The author(s). This article is licensed under a Creative Commons Attribution 4.0 International License, which permits use, sharing, adaptation, distribution and reproduction in any medium or format, as long as you give appropriate credit to the original author(s) and the source, provide a link to the Creative Commons license, and indicate if changes were made. The images or other third-party material in this article are included in the article's Creative Commons license, unless indicated otherwise in a credit line to the material. If material is not included in the article's Creative Commons license and your intended use is not permitted by statutory regulation or exceeds the permitted use, you will need to obtain permission directly from the copyright holder. To view a copy of this license, visit: <http://creativecommons.org/licenses/by/4.0/>

References

Alex, A. V., & Mukherjee, A. (2021). Review of recent developments (2018–2020) on acetylcholinesterase inhibition based biosensors for organophosphorus pesticides

- detection. *Microchemical Journal*, 161, 105779. <https://doi.org/10.1016/j.microc.2020.105779>
- Chauhan, N., & Pundir, C. S. (2011). An amperometric biosensor based on acetylcholinesterase immobilized onto iron oxide nanoparticles/multi-walled carbon nanotubes modified gold electrode for measurement of organophosphorus insecticides. *Analytica Chimica Acta*, 701(1), 66–74. <https://doi.org/10.1016/j.aca.2011.06.014>
- Das, S., & Adhya, T. K. (2015). Degradation of chlorpyrifos in tropical rice soils. *Journal of Environmental Management*, 152, 36–42. <https://doi.org/10.1016/j.jenvman.2015.01.025>
- Dewi, F. Y., Cahyono, S. T., Hilmi, F., Sanjaya, A. R., Hastuti, D. W., Pratiwi, N. I., Aliwarga, H. K., Prajitno, P., Ivandini, T. A., & Handoko, D. (2024). Electrochemical performance of gold nanoparticles decorated on Multi-walled Carbon Nanotube (MWCNT) Screen-printed Electrode (SPE). *ITM Web of Conferences*, 61, 01019. <https://doi.org/10.1051/itmconf/20246101019>
- Du, X., Wang, P., Fu, L., Liu, H., Zhang, Z., & Yao, C. (2020). Determination of chlorpyrifos in pears by raman spectroscopy with random forest regression analysis. *Analytical Letters*, 53(6), 821–833. <https://doi.org/10.1080/00032719.2019.1681439>
- Farsani, A. T., Arabi, M., & Shadkhast, M. (2021). Ecotoxicity of chlorpyrifos on earthworm *Eisenia fetida* (Savigny, 1826): Modifications in oxidative biomarkers. *Comparative Biochemistry and Physiology Part C: Toxicology & Pharmacology*, 249, 109145. <https://doi.org/10.1016/j.cbpc.2021.109145>
- Gaonkar, O., Nambi, I. M., & Suresh Kumar, G. (2019). Biodegradation kinetics of dichlorvos and chlorpyrifos by enriched bacterial cultures from an agricultural soil. *Bioremediation Journal*, 23(4), 259–276. <https://doi.org/10.1080/10889868.2019.1671791>
- Govindasamy, M., Mani, V., Chen, S. M., Chen, T. W., & Sundramoorthy, A. K. (2017). Methyl parathion detection in vegetables and fruits using silver@graphene nanoribbons nanocomposite modified screen printed electrode. *Scientific Reports*, 7. <https://doi.org/10.1038/srep46471>
- He, Y., Xiao, S., Dong, T., & Nie, P. (2019). Gold nanoparticles with different particle sizes for the quantitative determination of chlorpyrifos residues in soil by SERS. *International Journal of Molecular Sciences*, 20(11). <https://doi.org/10.3390/ijms20112817>
- Hongsibsong, S., Prapamontol, T., Xu, T., Hammock, B. D., Wang, H., Chen, Z. J., & Xu, Z. L. (2020). Monitoring of the organophosphate pesticide chlorpyrifos in vegetable samples from local markets in Northern Thailand by developed immunoassay. *International Journal of Environmental Research and Public Health*, 17(13), 1–14. <https://doi.org/10.3390/ijerph17134723>
- Ivandini, T. A., & Einaga, Y. (2017). Polycrystalline boron-doped diamond electrodes for electrocatalytic and electrosynthetic applications. *Chemical Communications*, 53(8), 1338–1347. <https://doi.org/10.1039/c6cc08681k>
- Ivandini, T. A., Watanabe, T., Matsui, T., Ootani, Y., Iizuka, S., Toyoshima, R., Kodama, H., Kondoh, H., Tateyama, Y., & Einaga, Y. (2019). Influence of Surface Orientation on Electrochemical Properties of Boron-Doped Diamond. *Journal of Physical Chemistry C*, 123(9), 5336–5344. <https://doi.org/10.1021/acs.jpcc.8b10406>
- Jankuloska, V., Karov, I., Pavlovska, G., & Buzlevski, I. (2017). Determination of Chlorpyrifos in Apple from the Resen Region. *Journal of Faculty of Food Engineering*, 16(1). <http://fia-old.usv.ro/fiajournal/index.php/FENS/article/view/466>
- Jepson, C., Murray, K., Jepson, P. C., Murray, K., Bach, O., Bonilla, M. A., & Neumeister, L. (2020). Selection of pesticides to reduce human and environmental health risks: a global guideline and minimum pesticides list. *Lancet Planet Health*, 4, e56–63. [https://doi.org/10.1016/S2542-5196\(19\)30266-9](https://doi.org/10.1016/S2542-5196(19)30266-9)
- Jiao, W., Ding, G., Wang, L., Liu, Y., & Zhan, T. (2022). Polyaniline functionalized CoAl-layered double hydroxide nanosheets as a platform for the electrochemical detection of

- carbaryl and isoprocarb. *Microchimica Acta*, 189(2). <https://doi.org/10.1007/s00604-022-05183-y>
- Karpouzas, D. G., & Singh, B. K. (2006). Microbial Degradation of Organophosphorus Xenobiotics: Metabolic Pathways and Molecular Basis. *Advances in Microbial Physiology*, 51(SUPPL.), 119–225. [https://doi.org/10.1016/S0065-2911\(06\)51003-3](https://doi.org/10.1016/S0065-2911(06)51003-3)
- Kaur, R., & Goyal, D. (2019). Toxicity and degradation of the insecticide monocrotophos. In *Environmental Chemistry Letters* (Vol. 17, Issue 3, pp. 1299–1324). Springer Verlag. <https://doi.org/10.1007/s10311-019-00884-y>
- Lee, K., Mazare, A., & Schmuki, P. (2014). One-dimensional titanium dioxide nanomaterials: Nanotubes. *Chemical Reviews*, 114(19), 9385–9454. https://doi.org/10.1021/CR500061M/ASSET/IMAGES/CR500061M.SOCIAL.IPEG_V03
- Li, A., Liu, X., Kong, J., Huang, R., & Wu, C. (2008). Chemiluminescence determination of organophosphorus pesticides chlorpyrifos in vegetables. *Analytical Letters*, 41(8), 1375–1386. <https://doi.org/10.1080/00032710802119228>
- Liu, T., Xu, M., Yin, H., Ai, S., Qu, X., & Zong, S. (2011). A glassy carbon electrode modified with graphene and tyrosinase immobilized on platinum nanoparticles for sensing organophosphorus pesticides. *Microchimica Acta*, 175(1–2), 129–135. <https://doi.org/10.1007/s00604-011-0665-5>
- Ma, P., Wang, L., Xu, L., Li, J., Zhang, X., & Chen, H. (2020). Rapid quantitative determination of chlorpyrifos pesticide residues in tomatoes by surface-enhanced Raman spectroscopy. *European Food Research and Technology*, 246(1), 239–251. <https://doi.org/10.1007/s00217-019-03408-8>
- Nagabooshanam, S., Roy, S., Mathur, A., Mukherjee, I., Krishnamurthy, S., & Bharadwaj, L. M. (2019). Electrochemical micro analytical device interfaced with portable potentiostat for rapid detection of chlorpyrifos using acetylcholinesterase conjugated metal organic framework using Internet of things. *Scientific Reports*, 9(1). <https://doi.org/10.1038/s41598-019-56510-y>
- Nandhini, A. R., Harshiny, M., & Gummadi, S. N. (2021). Chlorpyrifos in environment and food: A critical review of detection methods and degradation pathways. In *Environmental Science: Processes and Impacts* (Vol. 23, Issue 9, pp. 1255–1277). Royal Society of Chemistry. <https://doi.org/10.1039/d1em00178g>
- Norbert Adum, A., Gibson, G., Mwagandi Chimbevo, L., Sifuna Oshule, P., Essuman, S., & Nyabiba Asamba, M. (2021). Detection and Quantification of Chlorpyrifos in Soil, Milk, Dip Wash, Spray Race Residues Using High Performance Liquid Chromatography in Selected Dairy Farms in Kenya. *Science Journal of Analytical Chemistry*, 9(4), 88. <https://doi.org/10.11648/j.sjac.20210904.12>
- Pelit, F. O., Pelit, L., Ertaş, H., & Nil Ertaş, F. (2012). Development of a gas chromatographic method for the determination of Chlorpyrifos and its metabolite Chlorpyrifos-oxon in wine matrix. *Journal of Chromatography B: Analytical Technologies in the Biomedical and Life Sciences*, 904, 35–41. <https://doi.org/10.1016/j.jchromb.2012.07.006>
- Pino, F., Ivandini, T. A., Nakata, K., Fujishima, A., Merkoçi, A., & Einaga, Y. (2015). Magnetic enzymatic platform for organophosphate pesticide detection using boron-doped diamond electrodes. *Analytical Sciences*, 31(10), 1061–1068. <https://doi.org/10.2116/ANALSCI.31.1061/METRICS>
- Rachmawati, A., Sanjaya, A. R., Putri, Y. M. T. A., Gunlazuardi, J., & Ivandini, T. A. (2023). An acetylcholinesterase-based biosensor for isoprocarb using a gold nanoparticles-polyaniline modified graphite pencil electrode. *Analytical Sciences*, 39(6), 911–923. <https://doi.org/10.1007/s44211-023-00296-7>
- Rahmawati, I., Fiorani, A., Sanjaya, A. R., Irkham, Du, J., Saepudin, E., Einaga, Y., & Ivandini, T. A. (2024). Modification of boron-doped diamond electrode with polyaniline and gold particles to enhance the electrochemiluminescence of luminol for the detection of reactive oxygen species (hydrogen peroxide and hypochlorite). *Diamond and Related Materials*, 144. <https://doi.org/10.1016/j.diamond.2024.110956>

- Ramin, M., Omid, F., Khadem, M., & Shahtaheri, S. J. (2021). Combination of dispersive solid-phase extraction with dispersive liquid-liquid microextraction followed by high-performance liquid chromatography for trace determination of chlorpyrifos in urine samples. *International Journal of Environmental Analytical Chemistry*, 101(6), 810–820. <https://doi.org/10.1080/03067319.2019.1672670>
- Rawtani, D., Khatri, N., Tyagi, S., & Pandey, G. (2018). Nanotechnology-based recent approaches for sensing and remediation of pesticides. In *Journal of Environmental Management*, 206, 749–762. Academic Press. <https://doi.org/10.1016/j.jenvman.2017.11.037>
- Sinha, S. N., Rao, M. V. V., & Vasudev, K. (2012). Distribution of pesticides in different commonly used vegetables from Hyderabad, India. *Food Research International*, 45(1), 161–169. <https://doi.org/10.1016/j.foodres.2011.09.028>
- Talan, A., Mishra, A., Eremin, S. A., Narang, J., Kumar, A., & Gandhi, S. (2018). Ultrasensitive electrochemical immuno-sensing platform based on gold nanoparticles triggering chlorpyrifos detection in fruits and vegetables. *Biosensors and Bioelectronics*, 105, 14–21. <https://doi.org/10.1016/j.bios.2018.01.013>
- Tay, B. Y. P., & Wai, W. H. (2021). A gas chromatography–mass spectrometry method for the detection of chlorpyrifos contamination in palm-based fatty acids. *Journal of the American Oil Chemists' Society*, 98(8), 881–887. <https://doi.org/10.1002/AOCS.12512>
- Wahyuni, W. T., Ivandini, T. A., Saepudin, E., & Einaga, Y. (2016). Zanamivir immobilized magnetic beads for voltammetric measurement of neuraminidase at gold-modified boron doped diamond electrode. *AIP Conference Proceedings*, 1729. <https://doi.org/10.1063/1.4946958>
- Wei, M., Zeng, G., & Lu, Q. (2014). Determination of organophosphate pesticides using an acetylcholinesterase-based biosensor based on a boron-doped diamond electrode modified with gold nanoparticles and carbon spheres. *Microchimica Acta*, 181(1–2), 121–127. <https://doi.org/10.1007/s00604-013-1078-4>
- Williams, A. J. K., Norcross, A. J., Chandler, K. A., & Bingley, P. J. (2006). Non-specific binding to protein A Sepharose and protein G Sepharose in insulin autoantibody assays may be reduced by pre-treatment with glycine or ethanolamine. *Journal of Immunological Methods*, 314(1–2), 170–173. <https://doi.org/10.1016/j.jim.2006.06.003>
- Xue, R., Kang, T. F., Lu, L. P., & Cheng, S. Y. (2012). Immobilization of acetylcholinesterase via biocompatible interface of silk fibroin for detection of organophosphate and carbamate pesticides. *Applied Surface Science*, 258(16), 6040–6045. <https://doi.org/10.1016/j.apsusc.2012.02.123>
- Yang, L., Wang, G., & Liu, Y. (2013). An acetylcholinesterase biosensor based on platinum nanoparticles- carboxylic graphene-nafion-modified electrode for detection of pesticides. *Analytical Biochemistry*, 437(2), 144–149. <https://doi.org/10.1016/j.ab.2013.03.004>
- Yuan, Y., Chen, C., Zheng, C., Wang, X., Yang, G., Wang, Q., & Zhang, Z. (2014). Residue of chlorpyrifos and cypermethrin in vegetables and probabilistic exposure assessment for consumers in Zhejiang Province, China. *Food Control*, 36(1), 63–68. <https://doi.org/10.1016/j.foodcont.2013.08.008>
- Zamora-Sequeira, R., Starbird-Pérez, R., Rojas-Carillo, O., & Vargas-Villalobos, S. (2019). What are the main sensor methods for quantifying pesticides in agricultural activities? A review. In *Molecules* (Vol. 24, Issue 14). MDPI AG. <https://doi.org/10.3390/molecules24142659>
- Zhu, X., Li, W., Wu, R., Liu, P., Hu, X., Xu, L., Xiong, Z., Wen, Y., & Ai, S. (2021). Rapid detection of chlorpyrifos pesticide residue in tea using surface-enhanced Raman spectroscopy combined with chemometrics. *Spectrochimica Acta - Part A: Molecular and Biomolecular Spectroscopy*, 250. <https://doi.org/10.1016/j.saa.2020.119366>

Biographies of Authors

Abdul Basit, Department of Chemistry, Faculty of Mathematics and Natural Sciences, Universitas Indonesia, Depok, West Java 16424, Indonesia.

- Email: abdulbasit@ui.ac.id
- ORCID: N/A
- Web of Science ResearcherID: N/A
- Scopus Author ID: N/A
- Homepage: N/A

Ferinastiti, Department of Chemistry, Faculty of Mathematics and Natural Sciences, Universitas Indonesia, Depok, West Java 16424, Indonesia.

- Email: ferinastiti@ui.ac.id
- ORCID: N/A
- Web of Science ResearcherID: N/A
- Scopus Author ID: N/A
- Homepage: N/A

Yudistira Tesla, Singota Solutions; Bloomington, Indiana 47401, United States.

- Email: yudistiratesla.singota@gmail.com
- ORCID: 0000-0002-7034-1113
- Web of Science ResearcherID: N/A
- Scopus Author ID: 57192371075
- Homepage: N/A

Fadlinatin Naumi, Department of Chemical Engineering, Faculty of Engineering, Universitas Al-Khairiyah, Cilegon, West Java 42441, Indonesia.

- Email: fnaumi@unival-cilegon.ac.id
- ORCID: 0000-0002-9134-5279
- Web of Science ResearcherID: N/A
- Scopus Author ID: 57203435791
- Homepage: N/A